Mechanisms of Performance Enhancement With Force Feedback

Christopher R. Wagner Robert D. Howe
Division of Engineering and Applied Sciences, Harvard University, Cambridge, MA, USA
Email: cwagner@fas.harvard.edu, howe@deas.harvard.edu

Abstract

The addition of force feedback to virtual environments and teleoperators provides many benefits to the user. However, the mechanisms by which force feedback improves performance remain unknown. We present an experiment demonstrating that force feedback can provide a physical constraint to an operator's motion, passively restraining the hand and reducing error even before the operator can voluntarily respond to the force stimulus. Because of the presence of force feedback, the magnitude of unwanted incursions into a virtual wall were reduced by up to 80%, as compared to the case with no force feedback. We also propose that a second order mechanical model of the operator's hand can be used to quantify the benefits of force feedback. Using our model, we are able to account on average for over 95% of the variance in the force on the hand.

1. Introduction

The benefits of force feedback have been demonstrated in numerous environments and systems. Teleoperated tasks such as hazardous material handling and remote surgery have both shown an increase in performance with the addition of force feedback [1, 2]. Force feedback in a teleoperated blunt surgical dissection task has been shown to reduce forces applied by the instrument and to reduce unwanted motions that exceed a force threshold [3]. Virtual environments have also benefited when the user is presented with force information [4]. Force information may also serve to establish a more powerful feeling of presence in a remote environment [5]. However, the mechanisms by which force feedback improves performance have not been fully investigated. Knowledge of these mechanisms would allow optimal interface design and highlight tasks where force feedback would be most beneficial.

A common approach to analysis of force feedback is to create a model of the interacting limb or the interface mechanism. Finger and wrist impedance models have been developed to examine keyboard design [6] and haptic controller design [7] [8]. Limb impedances have also been found to change over time due to leaning effects and perceived task difficulty [9]. These impedance models, however, were derived at a fixed limb position and do not take into account the desired motion that is present when executing a task. Models of interface mechanisms have also been developed for use in conjunction with limb impedance to determine the optimal way to transmit forces. For example, models for bilateral telemanipulators are used to analyze stability while also minimizing the difference between remote and local forces [10]. Again, these models do not provide insight into the mechanisms by which forces improve performance. Some research has been presented on combining a teleoperator model and a hand impedance model to examine how forces help in teleoperation [11]; Daniel and McAree concluded that forces below 30 Hz act to transfer energy and forces above 30 Hz act as an information source. While these results are an important foundation, they do not relate the effects of force feedback to task characteristics and performance metrics.

We propose that a model of the operator's hand and the haptic interface mechanism combined with knowledge of the operator's desired motions can lead to insight into how force feedback improves operator performance. Our primary hypothesis is that force feedback exists as a physical constraint, passively restricting the motion of the operator. Secondly, we conjecture that a model of hand impedance can be used to derive the operator's desired motion trajectory in a task, allowing us to separate the passive benefit of force feedback that acts as a constraint from the informational benefit of force feedback that leads to voluntary motion changes. We present an experiment where users interact with a stylus attached to a robotic interface. Users move the stylus at a constant speed until encountering a tactile stimulus, either a vibration or a force resisting the direction of motion. Based upon their reaction time, we demonstrate that the force stimulus passively restricts the users motion before they can voluntarily react. Further, we show that a second order model of the hand/stylus system can be used to quantify the constraint and informational contributions of force feedback.

2. Methods And Materials

In this experiment, subjects execute a motion, and then reverse their motion upon feeling a haptic stimulus. In the 150 ms before the users can voluntarily respond to the stimulus [12], they will continue in the direction of the original motion. During this pre-voluntary time, when force feedback that resists the direction of motion is present, the hand will not travel as far as compared to the case where the stimulus is a vibration that provides no net force to the user. Because subjects cannot voluntarily respond during the pre-voluntary phase, we can also model the motion of the hand during that time using passive mechanical components. This model can be used to analyze the magnitude of the physical constraint and determine the user's voluntary motion after responding to the stimulus.

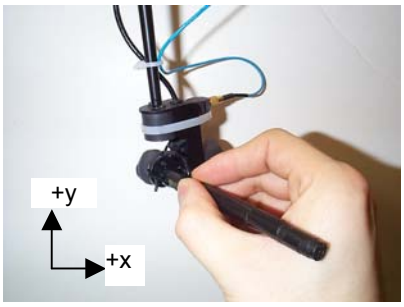

Fig. 1. Stylus grasp configuration

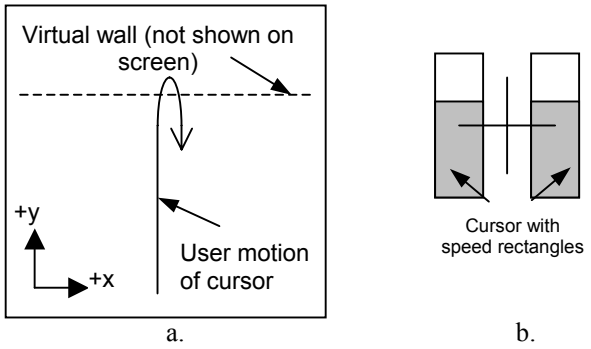

Fig. 2. (a) Diagram of workspace showing user motion. (b) Diagram of cursor with speed rectangles displaying a current speed above the desired speed target.

2.1. Experimental Design

A haptic interface device (Phantom 1.5, Sensable, Woburn, MA) was used to record the participant's trajectory data as well as provide haptic stimuli during the experiment [13]. We define the positive x direction to be to the right and positive y to be upward with respect to the user. Subjects grasped the stylus like a pen to control the motion of the tip of the stylus in the x, y plane (Fig. 1). A one-dimensional accelerometer (PiezoBeam 8630B50, Kistler, Amherst, NY) with a resolution of 0.005 m/s^2 was rigidly attached to the stylus gimbal to record accelerations in the y-dimension. Position and acceleration data were recorded at 1000 Hz for each trial.

Subjects were instructed to move the tip of an interface stylus upward (positive y direction) in a straight-line trajectory at a constant speed until encountering a 'wall.' The wall would be signified by the presence of either a force resisting the motion of the stylus or a vibration. Note that the only information on wall position presented to the user was through the haptic pathways. After contacting the wall, subjects were instructed to reverse their direction of motion as soon as possible and exit the wall.

A computer monitor provided feedback of the participant's current position in the x,y plane and velocity in the positive y direction. The position of the tip of the interface stylus was mapped to the position of a cursor with a scale factor of 1 (Figure 2a). A one to one mapping between stylus tip and cursor (i.e. a 1 cm motion of the stylus tip would move the cursor 1 cm on the screen) was used to remove any scaling effects. Velocity in the positive y-dimension was displayed using rectangles on either side of the cursor (Figure 2b). The height of the rectangles increased with increasing vertical speed, up to a maximum height. The desired constant velocity that participants were asked to move at corresponded to half of the maximum rectangle height. The workspace of the experiment in the x, y plane was 16 cm by 12 cm.

The path that the subject was asked to follow always began at the bottom center of the workspace. The wall stimulus would appear when the subject maintained a speed +/- 5% of the target speed of 40 mm/s for 100 ms. These numbers were determined through pilot studies to allow a reasonable success rate yet still restrict the participant's initial velocity to a narrow range. If the participant did not meet the speed criterion within the workspace, the trial was repeated. Subjects were given a training period where they practiced moving the stylus at a constant speed. All subjects were able to trigger the wall stimulus regularly (on average, one out of three attempts) within five minutes of training.

The motion of the participant's forearm was restricted through the use of a brace rigidly attached to the armrest of the participant's chair. The brace was used so that the wrist was the principal joint used to

move the stylus. To avoid any audio stimulus, particularly during the vibration trials, participants wore headphones playing noise in the frequency of the vibration.

2.2. Stimuli

Two types of stimuli were used in the experiment to represent a wall. The first type was a force vibration along the *x* dimension at 250 Hz with commanded amplitude of +/-1.0 N. The vibration frequency was chosen to maximally stimulate the rapidly adapting receptors in the fingertip. This stimulus was simply on or off depending on whether the subject was above or below the boundary of the wall. The second type of stimulus was a force in the negative *y* direction proportional to the distance traveled into the wall. This force is effectively a spring force with stiffness k_{wall}. Three force feedback gains of 33%, 67%, and 100% were used to scale the spring force during the experiment. Since the spring force was the only force encountered, the three levels of force feedback gains were equivalent to three different wall spring stiffnesses. The wall force can thus be expressed as

$$F_{wall} = -G_{FF} k_{wall} (y_{cursor} - y_{wall}) \qquad (1)$$

where y_{wall} is the *y* position of the start of the compliant wall, G_{FF} is the force feedback gain, k_{wall} is the wall stiffness, and y_{cursor} is the *y* position of the cursor. A wall stiffness of $k_{wall} = 0.54$ N/m was used in the experiment to give a perceptually relevant range of wall compliances.

The subject's motion was restricted to *x* ,*y* plane to simplify the workspace of the experiment to two dimensions and maintain the orientation of the accelerometer. A spring model (proportional error) was again used to generate the forces necessary to restrict motion in the *z* dimension

$$F_z = -k_z (z_{cursor}), \qquad (2)$$

with $k_z = 0.54$ N.

2.3. Hand model

A linear, second order system was used to model the impedance of the hand/stylus system. The model consists of a spring, mass, and damper as the link between a desired position input and an actual position output (Figure 3). This type of model was chosen due to its success in characterizing limb impedances [7] [14] and as an attempt to find a low order model that still encapsulates physical features relevant to force feedback. The model is also similar to one earlier proposed by Kuchenbecker et al. [8] who modeled the impedance of the wrist in a similar stylus grasp configuration. While the hand stylus system does not behave as a linear second order system over all ranges of input, a second order model has been shown to encapsulate the essential dynamics for the small excursions used here.

Writing a force balance for the hand/stylus model in contact with a compliant environment yields

$$k_{hand}(x_d - x_a) + b_{hand}(\dot{x}_d - \dot{x}_a) - m_{hand}\ddot{x}_a = F_w, \qquad (3)$$

where k_{hand}, b_{hand}, and m_{hand} are the parameters of the second order hand/stylus model, $x_d(t)$ is the desired hand motion from the central nervous system, $x_a(t)$ is the observed trajectory, and $F_w(t)$ is the wall force.

In order to differentiate between the passive benefits of force feedback and the changes in voluntary motion that result from force feedback, we estimate the desired trajectory of the hand (the commanded hand trajectory from the central nervous system) from the observed trajectories. We can do so in a four-step process using the model described above:

1) Find an estimate of the desired trajectory $x_d(t)$ for the first 150 ms after the user has encountered a stimulus by averaging all of the trajectories after a vibration stimulus occurred. Because the vibration applied no net force, the observed motion should closely match the desired motion.

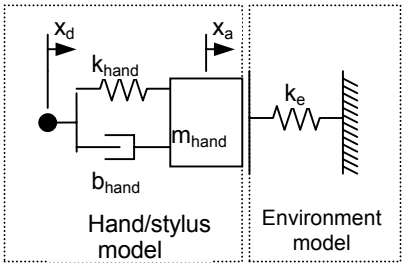

Fig. 3. Hand and environment models

2) Fit the parameters of a second order model (k_{hand}, b_{hand}, and m_{hand}) to the first 150 ms of observed position and force data for the force feedback cases using the above average as the desired trajectory. The fit parameters should be similar across all inputs since the user has not yet voluntarily responded.

3) Construct a mathematical description of the relationship between the input (desired trajectory) and

the output (observed trajectory) using the *average* of all fit model parameters for that subject.

4) Using the above relationship and assuming that the hand parameters remain relatively constant after the user responds to the stimulus, estimate the desired trajectory *after* 150 ms by applying the inverse of the relationship to the observed motion.

We now describe the steps of the above process in detail.

First, the parameters for the proposed hand model were estimated for each trial. The parameters can be fit using least squares by first expressing the force balance equation (3) at all sample times to be used for the fit as

$$Ap_{hand} = F_{wall} \tag{4}$$

where A is a concatenation of the system's states over n samples

$$A = \begin{bmatrix} x_d(t_0)-x_a(t_0) & \dot{x}_d(t_0)-\dot{x}_a(t_0) & \ddot{x}_a(t_0) \\ x_d(t_1)-x_a(t_1) & \dot{x}_d(t_1)-\dot{x}_a(t_1) & \ddot{x}_a(t_1) \\ \vdots & \vdots & \vdots \\ x_d(t_n)-x_a(t_n) & \dot{x}_d(t_n)-\dot{x}_a(t_n) & \ddot{x}_a(t_n) \end{bmatrix}, \tag{5}$$

p_{hand} is the column vector of hand parameters

$$p_{hand} = \begin{bmatrix} k_{hand} & b_{hand} & m_{hand} \end{bmatrix}^T \tag{6}$$

and F_{wall} is the column of wall forces at all sample times

$$F_{wall} = \begin{bmatrix} F_w(t_0) \\ F_w(t_1) \\ \vdots \\ F_w(t_n) \end{bmatrix}. \tag{7}$$

In these expressions, t_0 represents the time at which the user first contacts the wall and t_1 through t_n are the subsequent sample times (taken at 1 kHz). The time t_n = 150 ms was chosen so that the parameter estimates would only incorporate the passive hand dynamics and not any cognitive response to the force stimuli [12]. The stretch reflex is an active (although not cognitive) response that occurs in response to limb flexion at 30 ms [15]; we will consider the stretch reflex as part of the passive hand model as is commonly assumed [14]. Note that F_w is the commanded force to the Phantom; we assume that F_w matches closely with the force actually applied to the hand because the frequency content of F_w is within the bandwidth of the Phantom [13].

We will assume $\bar{x}_d(t)$ to be the average of all actual trajectories from t_0 to t_n for the vibration case. Because only vibrations were applied in that case and no net forces, the actual trajectory should closely follow the desired trajectory, assuming steady state prior to the stimulus, so $\bar{x}_a(t) = \bar{x}_d(t)$. This desired trajectory should be the same for all cases up to t_n, since users did not have a chance to voluntarily respond. The velocities $\dot{x}_d(t)$ and $\dot{x}_a(t)$ are found by differentiating high order (18 terms) polynomial fits to $\bar{x}_d(t)$ and $x_a(t)$, respectively. A polynomial solution is used to minimize high frequency noise in the derivative. The acceleration $\ddot{x}_a(t)$ is measured using the accelerometer. Once the data is expressed as (7), a least squares minimization is used to find the values of m_{hand}, b_{hand}, and k_{hand} that minimize the error $Ap_{hand} - F_w$. For our estimation, all hand parameter values were constrained to be non-negative.

An estimate of the desired trajectory for each trial can be constructed once the average hand parameters across all trials for a given subject have been found, assuming that k_{hand}, b_{hand}, and m_{hand} remain constant. The desired trajectory is found by solving the force balance (3) for $x_d(t)$ using Laplace transforms (see Appendix)

$$x_d(t) = deconv(x_a(t), h(t)) - g(t) \tag{8}$$

where $h(t)$ is the impulse response of the system model and $g(t)$ is the response due to initial conditions.

2.4. Experimental Design

Six people, aged 19 - 26 volunteered for the study. Participants described themselves as right handed with no known abnormalities in either hand.

The experiment conducted was a one factor, four level repeated measures design with an independent variable of stimulus type. The four levels of stimulus were vibratory, 33% force feedback gain, 67% force feedback gain, and 100% force feedback gain. Each subject completed 96 trials and received the same stimulus presentation order, in which the levels of stimulus were counterbalanced against order. The placement of the wall stimulus in the *y*-dimension, given that the subject had met the speed constraint, was also counterbalanced across trials.

3. Results

Figure 4 shows the average intrusion trajectory for each wall stimulus type for a typical subject. Each line is the average of 24 trajectories. We observe that as the force feedback gain is increased, average intrusion into the wall decreases. Note that the intrusion distance is reduced even before 150 ms when voluntary response can begin. This same trend is observed for all subjects up to 150 ms (Fig. 5) ($F(3,429) = 1562$, $p < 0.001$). The average maximum incursion reached in 150 ms decreases by an average of 80% across subjects. Because a reduction in incursion distance is occurring before voluntary response, for all subjects, force feedback is acting as a physical constraint to the motion of the hand.

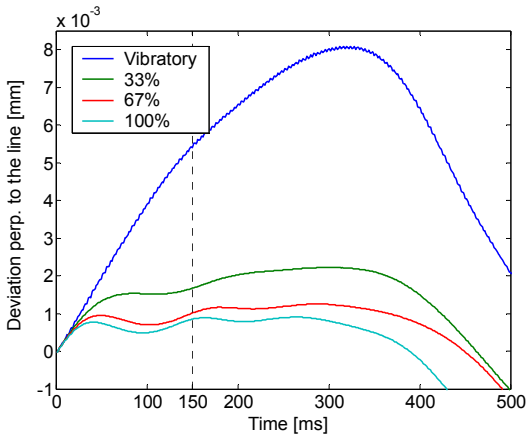

Fig. 4. Average trajectories for a typical subject

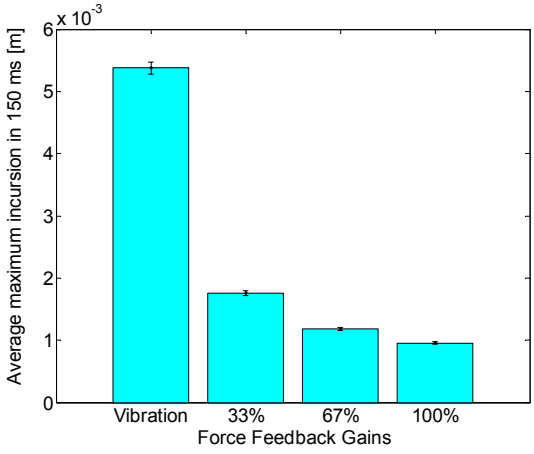

Fig. 5. Average maximum incursion in 150 ms for all subjects

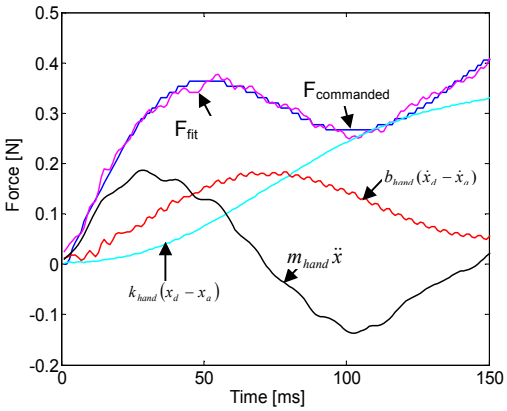

Fig. 6. Typical force fit up to 150 ms

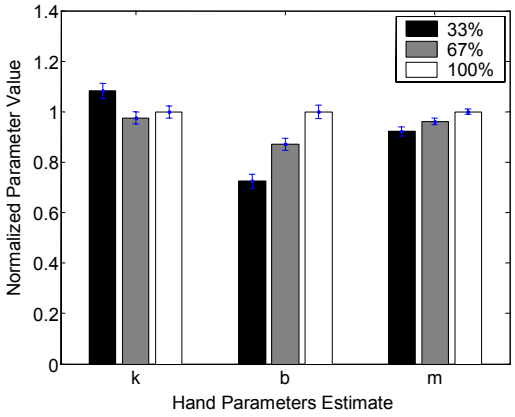

Fig. 7. Hand parameters estimated across subject and force feedback gain. Error bars show standard error.

A sample estimate of hand force over time is shown in Fig. 6, along with the forces that result from the individual elements. The small oscillations in the damping force are due to the velocity estimation process. The results of the hand parameter fits are shown in Table 1, with normalized values graphed in Fig. 7. Although trends in each of the normalized parameters were significant with respect to force feedback level (stiffness $F(2,286) = 4.77$, $p < 0.01$; damping $F(2,286) = 28.12$, $p < 0.001$; mass $F(2,286) = 7.17$, $p < 0.005$), the means for each parameter were within one standard deviation of one another. The average variance in force accounted for by the model (VAF), given by

$$VAF = 1 - \frac{mean[(F_{commanded} - F_{calculated})^2]}{\mathrm{var}(F_{commanded})}, \quad (9)$$

is shown in Table 2, with an average VAF of 96% across all trials.

Table 1. Average fit hand parameters per subject

Subject	Hand Parameters		
	k_{hand} [N/m]	b_{hand} [N-s/m]	m_{hand} [kg]
1	136.2	1.62	0.183
2	113.7	2.66	0.206
3	69.1	3.97	0.183
4	60.0	3.36	0.164
5	37.0	3.19	0.153
6	85.6	2.44	0.168
Mean	83.6	2.90	0.200

Table 2. Average variance in force accounted for

Subject	Force feedback levels			
	33%	*67%*	*100%*	*Mean*
1	95.60%	94.68%	96.36%	95.55%
2	97.14%	97.29%	96.49%	96.97%
3	97.92%	97.09%	95.90%	96.97%
4	97.24%	97.12%	97.35%	97.24%
5	95.76%	96.08%	96.59%	96.14%
6	95.64%	95.93%	95.95%	95.84%
Mean	96.55%	96.37%	96.44%	96.45%

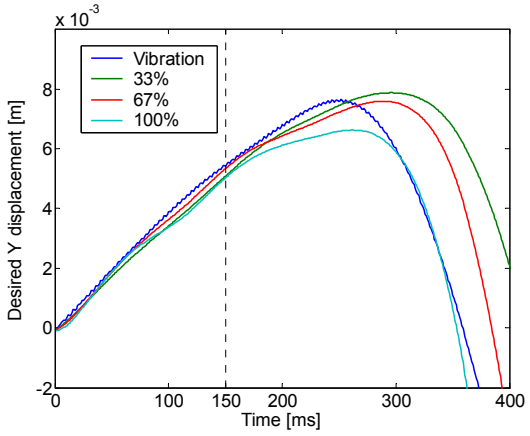

Fig. 8. Average estimated desired trajectories for a typical subject

Using the assumption that hand parameters are constant across all force feedback levels, the average of all fit hand parameters, per subject, were used to extract the desired trajectory $x_d(t)$ from each observed trajectory $x_a(t)$ including $t > 150$ ms. Figure 8 shows the average extracted desired motion for different levels of stimulus for a typical subject. Each line is again the average of 24 trials. Note that all trajectories are nearly collinear up until 150 ms, at which point they diverge. The average turnaround time (time when the desired trajectory reaches a maximum) for each subject and wall stimulus decreases by up to 70 ms for increasing force feedback level, not considering the vibration stimulus ($F(2,286) = 48.101$, $p < 0.001$) (Figure 9). The vibration stimulus condition was significantly different from the 100% case and the 33% case, shown using multiple t-test comparisons ($p < 0.005$, $p < 0.001$). However, all average turnaround times were found to be larger than the 100% condition average turnaround time, per subject.

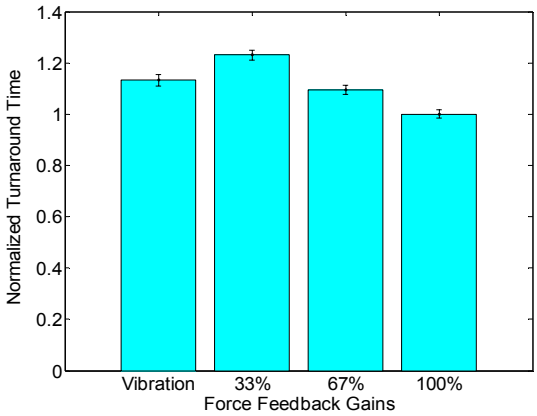

Fig. 9. Turnaround times of desired trajectories. Error bars show standard error.

4. Discussion

Our hypotheses were that force feedback causes a physical, passive error reduction before users can voluntarily respond to a contact stimulus, and that a physical model of the hand/interface system would allow an examination of the effects of force feedback magnitude on desired motion. Two different types of stimuli were used to examine the first hypothesis; one, a vibration that provided information of contact but no net force, the other a virtual spring with different levels of stiffness. In order to investigate the second hypothesis, a second order model was chosen to represent the hand/interface system. Our experiment was designed so that users were at a consistent, steady state condition before the stimulus in order to reduce variation between trials and increase the accuracy of fit for a low-order mechanical model.

We observe that force feedback does indeed act as a physical constraint to the motion of the hand/stylus system, where an increase in force feedback gain can lead to a dramatic reduction in incursion distance

before 150 ms. We also observe that a second order model works well at encapsulating the passive motion of the hand/stylus system, consistently accounting for the observed behavior across varying levels of input and force feedback gain. Using the second order model and assuming that hand parameters do not greatly change after 150 ms, we observe desired trajectories that match closely with the actual motion when there is no net force on the system. However, as force feedback gain increases, the turnaround time of the desired motion decreases for all subjects. Thus, the benefit of force feedback is two-fold: forces passively constrain the motion of the hand and provide information used to alter desired motion.

Several assumptions are made that lead to the above conclusion. The primary one is that the hand/stylus system behaves as a second order system, with desired position as input and actual position as output. Previous studies have attempted to fit low order models to various limb impedances and have met with varying success, with models breaking down when unable to encapsulate higher order effects, specifically those due to additional degrees of freedom [7] [8]. In our case, we have taken precautions to reduce variation between trials and restrict the dominant motion to the wrist. Even so, we observe a slight trend in the estimation of the damping parameter that varies with force feedback level. The main point, however, is that we are using the lowest order model that captures essential system dynamics. Using higher order models may achieve better fits, but at a cost of a large variation in the values of the fit parameters given the short time frame (<150 ms) used to fit. An additional assumption was that the hand parameters remained relatively constant after the 150 ms cutoff. This assumption was reasonable given that the estimates of $x_d(t)$ and the hand parameters m_{hand}, b_{hand}, and k_{hand} were relatively consistent across trials.

Several factors contributed to inaccuracies of the fit model, independent of the low model order. Primarily, the fitting technique requires the knowledge of both the desired trajectory and the output trajectory to extract the parameters. The desired trajectory varied between trials while the desired trajectory used to find m_{hand}, b_{hand}, and k_{hand} was an average of all the subject's trajectories in the vibration case. The discrepancy between the two could lead to inaccurate fits. Another source of error in the fitting technique is that, over the short fitting time, the magnitude of the forces due to the individual mechanical components are not always of the same order. Therefore, a large change in one parameter will not result in a large change in force relative to the force due to the other components, causing a range of acceptable fit values.

4.1 Benefits of Force Feedback

Based upon the results of the described experiment, we can make some observations concerning the nature of force feedback and its benefits. A primary observation is that there is a fundamental difference between force feedback and other forms of tactile feedback, such as vibration. Force feedback has the capability to reduce errors without requiring cognitive attention. The implications are that the benefits of force feedback can occur before 150 ms, and that taking advantage of force feedback does not necessarily increase mental workload. Vibration feedback, however, is strictly an information source, so the user has to devote attention to derive benefit and the error reduction benefit can only occur after 150 ms. It follows, then, that force feedback might be more useful than vibratory stimuli in situations where inaccurate motions can cause serious errors in a short time frame. Another possibility is in complex environments or difficult tasks where the user's mental workload is already high. A situation that fits both of these criteria is robotic surgery [16]. During a surgical procedure, surgeons often execute complex and physically demanding tasks with delicate tissues. If soft tissues generate significant constraint forces as hard surfaces do (a question for further investigation), force feedback would serve to reduce mental workload while passively restraining offending motions into sensitive tissues.

Another requirement for force feedback to provide this passive error reduction benefit is that forces must be generated in a direction opposite to the motion causing the error. Therefore, the passive benefit of force feedback is dependent on how 'error' is defined. An example of where force feedback's passive benefit would not help is when the user needs to exceed a force threshold to achieve a goal. Increasing the force feedback gain will only serve to make it more difficult to achieve the threshold. Severing tough connective tissue in a surgical task might be one example of this case. Further, the forces generated by force feedback need to be high enough to affect the motion of the hand/interface system for force feedback to achieve a passive benefit.

Using a model-based approach to analyzing the benefits of force feedback allows us to examine another possible benefit of force feedback, that of increased positioning resolution. A common example motivating the use of force feedback deals with attempting to move one's hand or a tool in a straight line. A free motion using only information-based forms of feedback, such as visual signals, is difficult and results in an imperfect straight line. However,

moving a tool, such as a pencil, in a straight line is trivial when using a ruler as a guide. The ruler constrains the motion of the pencil to lie exactly alongside the ruler. Using a ruler transforms a task requiring precise position control and mental effort into a simple task requiring the user only to push the pencil against the ruler. In a similar manner, force feedback can reduce the mental workload and positioning control accuracy needed when attempting to position a tool alongside an environmental structure. Returning to the robotic surgery example, if a surgeon needs to position a dissector along the edge of an organ, he or she can take advantage of the intrinsic stiffness of the organ to balance the force of contact, resulting in the dissector being positioned exactly next to the organ without exceeding a force threshold and damaging the organ.

A final benefit of a model of both the hand impedance and the desired motion in response to stimuli is that one can establish a design rule that relates force feedback gain, environmental stiffness, exploration speed, and maximum 'error'. For instance, if error is defined as maximum incursion into a structure (as it was with our experiment) and environment stiffness and force feedback gain are fixed, then the hand model and desired trajectory can be used to find the maximum exploration speed that will not result in exceeding a specified maximum incursion. Or, in the robotic surgery example, given typical exploration speeds of the surgeon, the model permits determination of the minimum force feedback gain required to guarantee that incursions never exceed a certain incursion threshold, for a given environment stiffness.

We have described an analysis of a constrained force feedback experiment using a low-order model. To extend these results to more general force feedback environments and still retain a quantitative predictive ability, the models of the hand/interface system and the environment should be augmented. The hand system, for instance, will behave differently along different axes of motion [17] and at different points in the robot workspace [13]. Also, not all environments can be modeled as a simple spring. An example of a more complex environment would be surgery, where tissues are viscoelastic and highly nonlinear [18]. Finally, desired trajectories may be different for different levels of force on the hand. Choosing different force feedback gains, however, can bring a range of environment forces and stiffnesses into the force levels on the hand encountered in our described experiment.

5. Acknowledgments

This work was supported in part by NSF grant EEC-9731748 and an NSF Graduate Research Fellowship for the first author.

The authors would like to thank Ryan Beasley, Doug Perrin, Paul Novotny, Amy Kerdok, Ross Feller, and all the members of the Harvard BioRobotics Lab for their perceptive comments and constructive criticisms.

6. References

[1] T. B. Sheridan, *Telerobotics, automation, and human supervisory control*. Cambridge, Mass.: MIT Press, 1992.

[2] A. Kazi, "Operator performance in surgical telemanipulation," *Presence*, vol. 10, pp. 495-510, 2001.

[3] C. R. Wagner, N. Stylopoulos, and R. D. Howe, "The role of force feedback in surgery: analysis of blunt dissection," presented at Proceedings 10th Symposium on Haptic Interfaces for Virtual Environment and Teleoperator Systems. HAPTICS 2002, Orlando, FL, USA

[4] F. Tendick, M. Downes, T. Goktekin, M. C. Cavusoglu, D. Feygin, X. Wu, R. Eyal, M. Hegarty, and L. W. Way, "A virtual environment testbed for training laparoscopic surgical skills," *Presence*, vol. 9, pp. 236-55, 2000.

[5] E.-L. Sallnas, K. Rassmus-Grohn, and C. Sjostrom, "Supporting presence in collaborative environments by haptic force feedback," *ACM Transactions on Computer-Human Interaction*, vol. 7, pp. 461-76, 2000.

[6] J. T. Dennerlein, Y. Zhou, and Becker, "Predicting exposure of the finger flexor muscle and tendon to dynamic loads during finger tapping," presented at Exposure Assessment in Epidemiology and Practice, Göteborg, Sweden, 2001.

[7] A. Z. Hajian and R. D. Howe, "Identification of the mechanical impedance at the human finger tip," *Transactions of the ASME. Journal of Biomechanical Engineering*, vol. 119, pp. 109-14, 1997.

[8] K. J. Kuchenbecker, J. G. Park, and G. Niemeyer, "Characterizing the human wrist for improved haptic interaction," presented at International Mechanical Engineering Congress and Exposition, Washington, D.C. USA, 2003.

[9] Y. Matsuoka and R. D. Howe, "Hand Impedance Change during Learning of a Novel Contact Task," presented at World Congress on Medical Physics and Biomedical Engineering, 2000.

[10] B. Hannaford and P. Fiorini, "A detailed model of bi-lateral teleoperation," presented at Proceedings of the 1988 IEEE International Conference on Systems, Man, and Cybernetics (IEEE Cat. No.88CH2556-9), Beijing, China, 1988.

[11] R. W. Daniel and P. R. McAree, "Fundamental limits of performance for force reflecting teleoperation," *International Journal of Robotics Research*, vol. 17, pp. 811-830, 1998.

[12] K. R. Boff and J. E. Lincoln, "Engineering Data Compendium: Human perception and performance," vol. 3. Wright-Patterson Air Force Base, Ohio, 1988.

[13] M. C. Cavusoglu, D. Feygin, and F. Tendick, "A Critical Study of the Mechanical and Electrical Properties of the PHANToM Haptic Interface and Improvements for High Performance Control," *Presence: Teleoperators and Virtual Environments*, vol. 11, pp. pp. 555 - 568, 2002.

[14] R. E. Kearney and I. W. Hunter, "System identification of human joint dynamics," *Crit Rev Biomed Eng*, vol. 18, pp. 55-87, 1990.

[15] T. A. McMahon, *Muscles, Reflexes, and Locomotion*. Princeton, New Jersey: Princeton University Press, 1984.

[16] R. D. Howe and Y. Matsuoka, "Robotics for Surgery," *Annual Review of Biomedical Engineering*, vol. 1, pp. 211-240, 1999. An expanded version is available as a tech report at http://biorobotics.harvard.edu/pubs/Matsuoka-howe03.pdf

[17] F. Tendick and L. Stark, "Analysis of the surgeon's grasp for telerobotic surgical manipulation," presented at Images of the Twenty-First Century. Proceedings of the Annual International Conference of the IEEE Engineering in Medicine and Biology Society (Cat. No.89CH2770-6), New York, NY, USA, 1989.

[18] Y. C. Fung, *Biomechanics: Mechanical Properties of Living Tissues*, 2nd ed. New York, NY: Springer-Verlag, 1993.

7. Appendix

Taking the Laplace transform of (3)

$$\begin{aligned} &k_{hand}(X_d(s)-X_a(s)) \\ &+b_{hand}(sX_d(s)-x_d(0)-sX_a(s)+x_a(0)) \\ &-m_{hand}(s^2X_a(s)-sx_a(0)-\dot{x}_a(0))=k_eX_a(s) \end{aligned} \tag{10}$$

Knowing the initial conditions $x_a(0) = 0$ because we define the wall's position to be at 0, and $x_d(0) = 0$ because we assume the system is in steady state before the wall, we can solve for $X_d(s)$,

$$X_d(s)=X_a(s)\left(\frac{k_h+k_e+b_{hand}s+m_{hand}s^2}{k_h+b_{hand}s}\right)-\frac{m_{hand}\dot{x}_a(0)}{k_h+b_{hand}s} \tag{11}$$

we can then rewrite $X_d(s)$ as

$$X_d(s)=X_a(s)\left(\frac{1}{H(s)}\right)-G(s) \tag{12}$$

where

$$H(s)=\frac{b_{hand}}{m_{hand}}\left(\frac{s+\alpha}{s^2+2\zeta\omega_n s+\omega_n{}^2}\right) \tag{13}$$

$$\omega_n=\sqrt{\frac{k_h+k_e}{m_{hand}}},\ \zeta=\frac{b_{hand}}{2m_{hand}\omega_n},\ \alpha=\frac{k_{hand}}{b_{hand}} \tag{14}$$

$$G(s)=\frac{m_{hand}\dot{x}_a(0)}{k_h+b_{hand}s}. \tag{15}$$

Solving for $h(t)$ by taking the inverse Laplace transform of (13)

$$h(t)=\beta e^{-\zeta\omega_n t}\sin\left[\omega_n\sqrt{1-\zeta^2}\,t+\tan^{-1}\left(\frac{\omega_n\sqrt{1-\zeta^2}}{\alpha-\zeta\omega_n}\right)\right] \tag{16}$$

where

$$\beta=\frac{b_{hand}}{m_{hand}\omega_n}\sqrt{\frac{\alpha^2-2\alpha\zeta\omega_n+\omega_n{}^2}{1-\zeta^2}}. \tag{17}$$

Similarly, solving for $g(t)$

$$g(t)=\frac{m_{hand}}{b_{hand}}\dot{x}_a(0)e^{\frac{-k_h}{b_{hand}}t}. \tag{18}$$

Because division in the frequency domain is the same as deconvolution in the time domain

$$x_d(t)=deconv(x_a(t),h(t))-g(t). \tag{19}$$